Molecular Vision 2020; 26:204-215 <http://www.molvis.org/molvis/v26/204>
Received 9 October 2019 | Accepted 16 March 2020 | Published 18 March 2020

p62/Sequestosome 1 levels increase and phosphorylation is altered in Cx50D47A lenses, but deletion of p62/sequestosome 1 does not improve transparency

Oscar Jara, Hubert Mysliwiec, Peter J. Minogue, Viviana M. Berthoud, Eric C. Beyer

Department of Pediatrics, University of Chicago, Chicago, IL

Purpose: p62/Sequestosome 1 (p62) is a stress-induced protein that is involved in several different intracellular pathways, including regulation of aspects of protein degradation. p62 levels are elevated in several types of cataracts. We investigated whether levels of p62 and its phosphorylation were altered in the lenses of Cx50D47A mice, which express a mutant of connexin50 (Cx50) that leads to cataracts and impaired lens differentiation. To evaluate the importance of p62 in the lens defects caused by a connexin50 mutant, we also examined the effect of deleting *p62* in homozygous Cx50D47A mice.

Methods: Protein levels were determined with immunoblotting. Mouse lenses were examined with dark-field illumination microscopy. Intensities of the opacities and lens equatorial diameters were quantified using ImageJ. Nuclei and nuclear remnants were detected with fluorescence microscopy of lens sections stained with 4′,6-diamino-2-phenylindole dihydrochloride (DAPI).

Results: Levels of total p62 were increased in the lenses of homozygous Cx50D47A mice compared to those of the wild-type animals. The ratio of p62 phosphorylated at threonine-269/serine-272 (T269/S272) to total p62 was significantly decreased, whereas the ratio of p62 phosphorylated at serine-349 (S349) to total p62 was significantly increased in lenses of homozygous Cx50D47A mice. However, deletion of *p62* did not affect the sizes of the lenses or the severity of their cataracts in homozygous Cx50D47A mice. Deletion of *p62* did not improve connexin50 or connexin46 levels. Moreover, deletion of *p62* did not change the levels of crystallins, histone H3, the mitochondrial import receptor subunit TOM20 homolog, or the abundance of nuclei and nuclear fragments in the lenses of homozygous Cx50D47A mice. Homozygous deletion of *p62* led to an 84% increase in the levels of ubiquilin 2, but did not significantly affect the levels of ubiquilin 1 or ubiquilin 4.

Conclusions: Although homozygous Cx50D47A lenses have increased levels of p62, a specific reduction in p62 phosphorylation at T269/S272, and a specific increase in p62 phosphorylation at S349, this protein is not a critical determinant of the severity of the abnormalities of these lenses (reduced growth or differentiation and cataracts). The lens may utilize redundant or compensatory systems (such as changes in levels of ubiquilin 2) to compensate for the lack of p62 in homozygous Cx50D47A lenses.

A substantial proportion of congenital cataracts result from mutations in genes expressed in the lens, including those encoding crystallins, transmembrane proteins, and transcription factors (Cat-Map) [1]. The genes encoding the lens gap junction proteins, connexin46 (Cx46) and connexin50 (Cx50), are prominent among the cataract-linked genes [2,3]. To elucidate the mechanisms by which connexin mutations lead to cataracts, we have been studying mouse models that mimic the mutations identified in human pedigrees with inherited congenital cataracts. One of the most studied of these models is the Cx50D47A mouse [4-9]. Heterozygous and homozygous mice have smaller lenses than their wild-type littermates, and they develop nuclear cataracts [4-6]. Cx50D47A lenses have reduced levels of Cx46 and Cx50, leading to reduced gap junctional communication between the lens fiber cells and impaired lens circulation [6,9]. In Cx50D47A lenses, the degradation of nuclei and cytoplasmic organelles that normally accompanies lens differentiation is impaired [6], and some aspects of the endoplasmic reticulum (ER) stress or unfolded protein response are activated [7]. Cellular stresses and abnormalities of protein and organelle degradation have been implicated in the pathogenesis of cataracts of many different etiologies.

We suspected that the alterations of the Cx50D47A lenses (and possibly other types of cataracts) might be mediated (at least in part) by p62/sequestosome 1 (p62) which is a stress-inducible protein that can act as a signaling hub for several different intracellular pathways, including vesicular trafficking, autophagy, protein degradation, cell proliferation, inflammation, and antioxidant responses [10-13]. Previous

Correspondence to:_Eric C. Beyer, Department of Pediatrics University of Chicago, 900 East 57th St. KCBD-5152, Chicago, IL 60637 Phone: (773) 834-1498; FAX: (773) 834-1329; email: ebeyer@peds.bsd.uchicago.edu

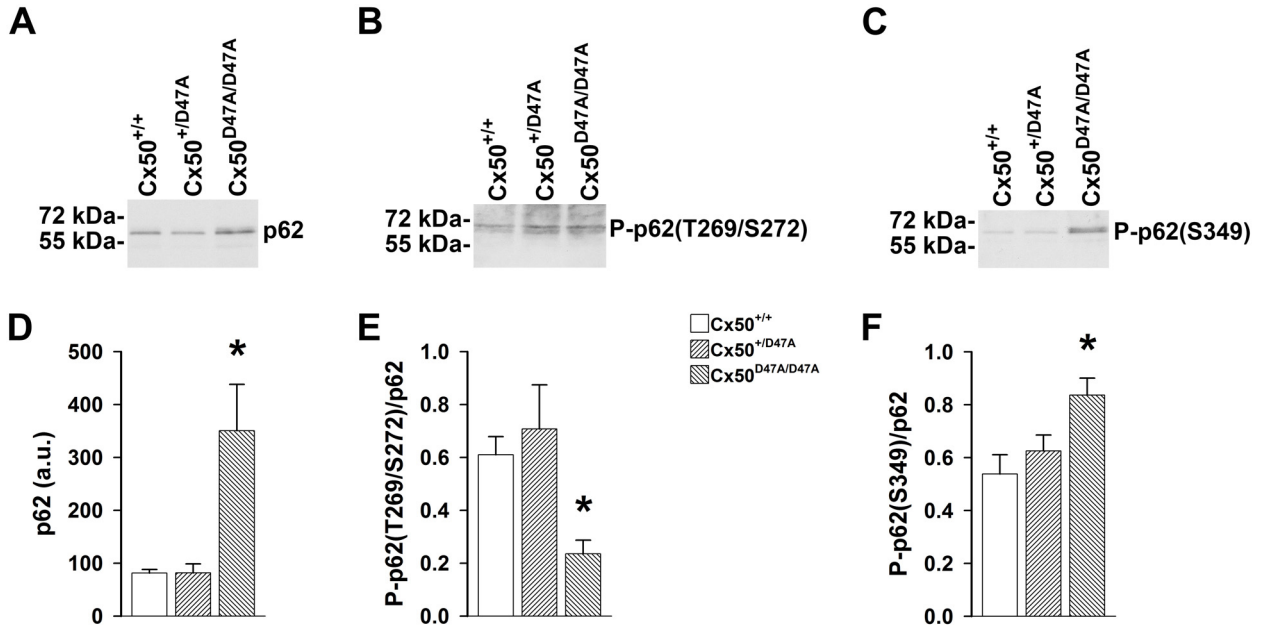

Figure 1. Levels of total p62 and its phosphorylated forms are altered in lenses of homozygous Cx50D47A mice. **A**–**C**: Representative immunoblots show levels of total p62 (**A**), p62 phosphorylated at threonine-269/serine-272 (P-p62(T269/S272) (**B**), and p62 phosphorylated at serine-349 (P-p62(S349) (**C**) in lens homogenates prepared from 1-month-old wild-type, or heterozygous or homozygous Cx50D47A mice. The migration positions of the molecular mass markers are indicated on the left. **D**: The graph shows the densitometric values of the immunoreactive bands of total p62. Data are presented as the mean (bar) + standard error of the mean (SEM; n = 6 sets) in arbitrary units (a.u.). **E**, **F**: The graphs show the ratio of p62 phosphorylated at T269/S272 to total p62 (**E**) and the ratio of p62 phosphorylated at S349 to total p62 (**F**) calculated from the densitometric values of the immunoreactive bands. Data are presented as the mean (bar) + SEM; n = 6 sets for P-p62(T269/S272), and n = 3 sets for P-p62(S349). Asterisks denote statistically significant differences from wild-type lenses ($p<0.05$).

studies have implicated p62 in cataractogenesis. Levels of p62 are elevated in the lenses of αB-crystallin R120G mice [14,15]. *p62* mRNA levels are increased in mice heterozygous for the lens opacity (*Lop*) mutation in aquaporin 0 (*Mip*) [16]. Transgenic mice expressing a dominant negative fibroblast growth factor receptor develop protein aggregates in their lenses and have increased levels of p62 [17]. We previously found that p62 associates with degradation-resistant accumulations of a different Cx50 mutant (Cx50P88S) when it was studied in cultured cells [18]. Although p62 phosphorylation has not been studied in relation to cataracts, this post-translational modification is important in modulating p62 functions in other tissues. As examples, phosphorylation of p62 on serine-349 (S349) affects selective autophagy and leads to activation of the Keap1-Nrf2 antioxidant response in hepatocytes [19], and double phosphorylation of p62 on threonine-269/serine-272 (T269/S272) facilitates cellular entry into and exit from mitosis in lung adenocarcinoma cells [20]. In the present study, we examined the alterations of p62 levels and the phosphorylation of p62 in the lenses of Cx50D47A mice, and we studied the consequences of deleting *p62* on lens size, cataractogenesis, and the levels of several lens proteins in these animals.

METHODS

Antibodies: Rabbit polyclonal anti-p62/SQSTM1 antibody (P0067; lot # 126M4796V) was obtained from Sigma (St. Louis, MO). Rabbit polyclonal anti-phospho-SQSTM1/p62 (Thr269/Ser272) (13121S; lot # 2), anti-phospho-SQSTM1/p62 (Ser349) (95697S; lot # 1), and anti-histone H3 (4499S; lot # 9) were obtained from Cell Signaling Technology (Danvers, MA). Polyclonal anti-Ubiquilin1 (PA5-22174; lot # UL2903952C) was obtained from Thermo Fisher Scientific (Waltham, MA). Mouse monoclonal anti-Ubiquilin2 (MABN763; lot # 3035872) was obtained from Millipore-Sigma (Burlington, MA). Mouse monoclonal anti-Ubiquilin4 (sc-136145; lot # E1716) and rabbit polyclonal anti–β-crystallin (sc-48335; lot # A1706) and anti-translocase of outer mitochondrial membrane 20 (TOM20) (sc-11415; lot # D1613) were obtained from Santa Cruz Biotechnology, Inc. (Dallas, TX). Affinity-purified rabbit polyclonal anti-Cx46 intracellular loop and anti-Cx50 C-terminus antibodies have been previously described [6,21]. Other primary antibodies (to cellular compartments and crystallins) and secondary antibodies were the same as those used in other recent studies from our laboratory [22,23]. Rabbit polyclonal

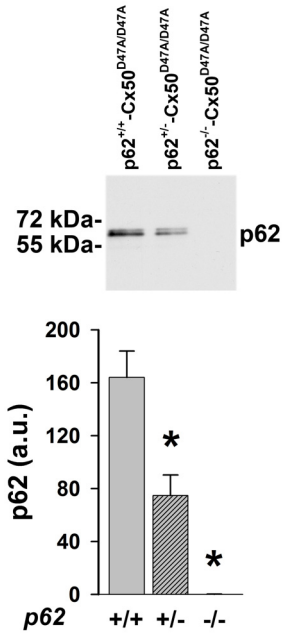

Figure 2. *p62* deletion was confirmed in lenses of *p62* null mice interbred with homozygous Cx50D47A mice. Representative immunoblot shows p62 levels in lens homogenates from 1-month-old homozygous Cx50D47A littermates that were wild-type for *p62* ($p62^{+/+}$-$Cx50^{D47A/D47A}$) or heterozygous ($p62^{+/-}$-$Cx50^{D47A/D47A}$) or homozygous ($p62^{-/-}$-$Cx50^{D47A/D47A}$) *p62* null. The migration positions of the molecular mass markers are indicated on the left. The graph shows the mean (bar) + standard error of the mean (SEM) of the densitometric values of the immunoreactive bands obtained from three biologic replicates expressed in arbitrary units (a.u.). Asterisks denote statistically significant differences from $p62^{+/+}$-$Cx50^{D47A/D47A}$ values ($p<0.05$).

anti–αA (SPA-221; lot # 10010805) and anti–αB-crystallin (SPA-223; lot # 08011134) antibodies were obtained from Enzo Life Sciences (Farmingdale, NY). Rabbit polyclonal anti–γ-crystallin antibodies were a kind gift from Dr Samuel Zigler (Wilmer Eye Institute at Johns Hopkins University, Baltimore, MD). Horseradish peroxidase–conjugated goat AffiniPure anti-rabbit immunoglobulin G (IgG; H+L; 111–035–144; lot # 123520 and 135724) and horseradish peroxidase–conjugated goat AffiniPure F(ab')2 fragment goat anti-mouse IgG, F(ab')2 fragment-specific (115–036–072; lot # 111686 and 135721) antibodies were obtained from Jackson ImmunoResearch (West Grove, PA).

Animals: Cx50D47A (also known as *No2* or ENU-326) mice [4] were maintained in the C3H line as previously described [6]. *p62* null mice [24] were obtained from Dr. Toru Yanagawa (University of Tsukuba, Tsukuba, Japan). These *p62* knockout mice were bred into the C3H line for six generations before the experiments were performed. Microscopic examination of the lenses of these animals in our laboratory showed no apparent differences in size or transparency compared to wild-type mice of the same strain. Heterozygous *p62* null ($p62^{+/-}$) mice were mated with homozygous Cx50D47A ($Cx50^{D47A/D47A}$) mice to generate heterozygous *p62* knockout mice that were homozygous for the Cx50 mutation ($p62^{+/-}$-$Cx50^{D47A/D47A}$). Mice of this genotype from different litters were mated to obtain homozygous Cx50D47A mice that were wild-type for *p62* or heterozygous or homozygous for *p62* deletion. All animal procedures followed the University of Chicago Animal Care and Use Committee guidelines and were conducted in accordance with the ARVO Statement for the Use of Animals in Ophthalmic and Vision Research and with the National Institutes of Health regulations.

Quantification of lens sizes and opacities: Dark-field photomicrographs of lenses from 1-month-old mouse littermates containing all genotypes (referred to as a set) were obtained using a Zeiss Stemi-2000C dissecting scope (Carl Zeiss, München, Germany). The same settings (i.e., magnification, illumination, and exposure time) were used to photograph all lenses within each set. Cataracts (opacities) were quantified in photomicrographs by integrating the gray values over a circular region of interest (of identical size for all images) using NIH ImageJ software (https://imagej.nih.gov/ij/) as previously performed [8,23]. These integrated opacity data are reported in arbitrary units. Equatorial diameters were determined from the lens photomicrographs using NIH ImageJ software. The opacities and the diameters were measured in both lenses of each mouse (unless one of the lenses was damaged during dissection), and the reported values are the averages of the measurements of the two lenses for each mouse.

Staining of lens nuclei: Lenses from 1-month-old mice were fixed in 4% paraformaldehyde in PBS (137 mM NaCl, 2.7

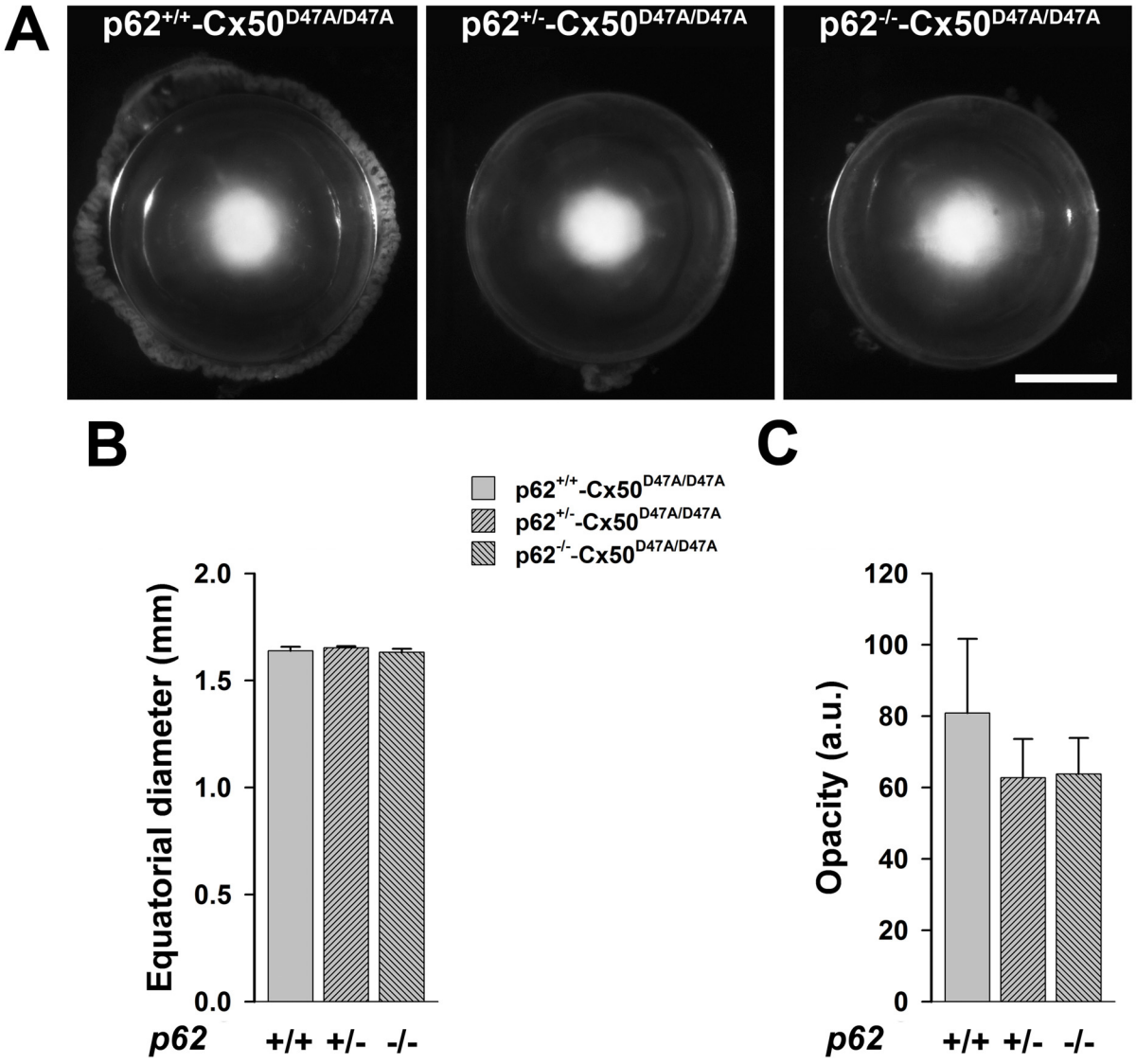

Figure 3. The sizes and opacities of homozygous Cx50D47A lenses are not affected by the deletion of *p62*. **A**: Dark-field photomicrographs of lenses from 1-month-old homozygous Cx50D47A littermates that were wild-type for *p62* (*p62*$^{+/+}$-Cx50$^{D47A/D47A}$) or heterozygous (*p62*$^{+/-}$-Cx50$^{D47A/D47A}$) or homozygous (*p62*$^{-/-}$-Cx50$^{D47A/D47A}$) *p62* null. **B**: The graph shows the equatorial diameters (in mm) determined from dark-field photomicrographs of lenses from homozygous Cx50D47A mice that were wild-type for *p62* (*p62*$^{+/+}$-Cx50$^{D47A/D47A}$) or heterozygous (*p62*$^{+/-}$-Cx50$^{D47A/D47A}$) or homozygous (*p62*$^{-/-}$-Cx50$^{D47A/D47A}$) *p62*-null. **C**: The graph shows the quantification of the integrated densities of the cataracts (opacities) from *p62*$^{+/+}$-Cx50$^{D47A/D47A}$, *p62*$^{+/-}$-Cx50$^{D47A/D47A}$ or *p62*$^{-/-}$-Cx50$^{D47A/D47A}$ lenses in arbitrary units (a.u.). Data in **B** and **C** are presented as the mean (bar) + standard error of the mean (n = 3 sets). Scale bar: 600 µm.

mM KCl, 10 mM Na_2HPO_4, 2 mM KH_2PO_4, pH 7.4). After several rinses, the lenses were transferred to 30% sucrose in PBS and left at 4 °C until they sank. Cryostat sections (18 µm) were obtained and incubated with 4′,6-diamino-2-phenylindole dihydrochloride (DAPI; Invitrogen, Carlsbad, CA) to stain the nuclei. Specimens were observed using an epifluorescence Axioplan 2 microscope (Carl Zeiss). Images (10X magnification) were acquired with a Zeiss AxioCam digital camera using Zeiss AxioVision software. Photomontages were constructed, and composite figures were assembled using Adobe Photoshop CS3 Extended (Adobe Systems, Inc., San Jose, CA).

Immunoblotting: Proteins were detected and quantified with immunoblotting of whole lens homogenates prepared from the two lenses of 1-month-old mice as described by Minogue et al. [23]. Samples were prepared by homogenizing the 2

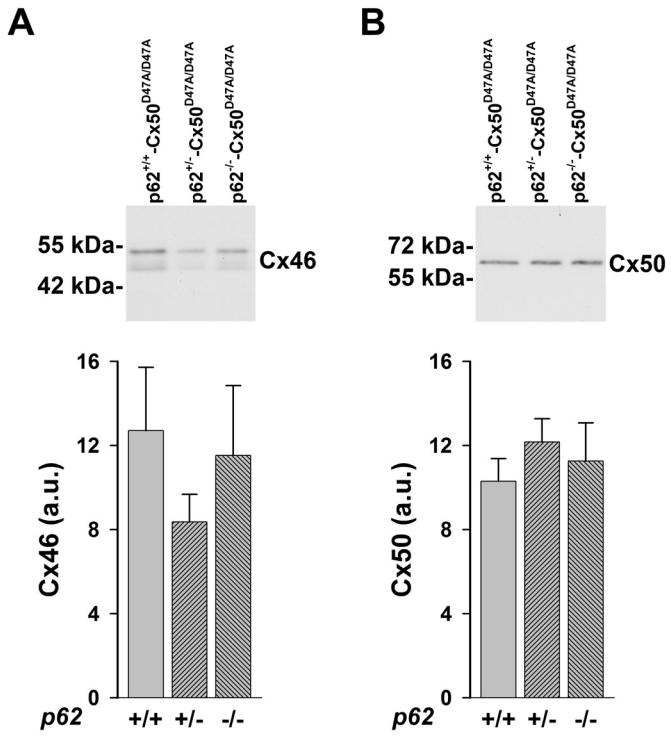

Figure 4. Deletion of *p62* in $Cx50^{D47A/D47A}$ mice does not alter levels of lens fiber connexins. **A**, **B**: Top panels, Immunoblots of Cx46 (**A**) and Cx50 (**B**) in lens homogenates prepared from 1-month-old $Cx50^{D47A/D47A}$ mice that were wild-type for *p62* ($p62^{+/+}$-$Cx50^{D47A/D47A}$) or heterozygous ($p62^{+/-}$-$Cx50^{D47A/D47A}$) or homozygous ($p62^{-/-}$-$Cx50^{D47A/D47A}$) *p62* null. The migration positions of the molecular mass markers are indicated on the left. The graphs at the bottom show the quantification of the density of the Cx46 (**A**) and Cx50 (**B**) immunoreactive bands in arbitrary units (a.u.). Data are presented as the mean (bar) + standard error of the mean (n = 6 sets for Cx46; n = 3 sets for Cx50).

lenses from each mouse in PBS containing 4 mM EDTA, 2 mM phenylmethyl sulfonylfluoride, 20 mM NaF, 10 mM Na_3VO_4 and cOmplete EDTA-free protease inhibitor cocktail (Roche Applied Science, Indianapolis, IN) using a glass-glass homogenizer followed by sonication. Protein concentrations were determined using the Bio-Rad Protein Assay Dye Reagent Concentrate (Bio-Rad, Hercules, CA). Aliquots from lens homogenates containing equal amounts of total protein were loaded in each lane and resolved by electrophoresis on sodium dodecyl sulfate-polyacrylamide (SDS-PAGE) gels. Gels were then blotted to Immobilon P membranes (Millipore, Bedford, MA) using a wet transfer apparatus. Then, the membranes were stained with Ponceau S (to verify equal electrotransfer of the proteins) before being subjected to immunoblotting as previously described [7,23]. The bands obtained in at least three independent experiments (i.e., biological replicates) were quantified by densitometry using a rectangular box that encompassed the immunoreactive band(s) using Adobe Photoshop CS3.

Statistical analysis: Raw data obtained from heterozygotes and homozygotes were compared to the raw data obtained from wild-type (or control) littermates to assess statistical significance using the Student *t* test. Statistical analysis was performed using Microsoft Excel. Graphs were prepared using SigmaPlot 10.0 (Systat Software, Inc.). A p value of less than 0.05 was considered statistically significant. The sets of littermates containing all genotypes (statistical n) totaled at least three for each type of data presented.

RESULTS

Levels of p62 and phosphorylated p62 are altered in homozygous Cx50D47A lenses: We used immunoblotting to examine the levels of total p62 in lenses of wild-type mice and mice that were heterozygous or homozygous for the Cx50D47A mutation (Figure 1A–C). Quantitation of blots showed that total p62 levels in lens homogenates did not differ significantly between wild-type and Cx50D47A heterozygotes, but the total p62 levels were more than twice as high in homozygotes ($Cx50^{D47A/D47A}$) as in wild-type mice (Figure 1D).

We also used immunoblotting to assess the levels of p62 phosphorylated at T269/S272 (P-p62(T269/S272)) and p62 phosphorylated at S349 (P-p62(S349)) in these lenses (Figure 1B,C). Although the ratio of P-p62(T269/S272) to total p62 did not differ between lenses from wild-type mice and mice that were heterozygous for the Cx50D47A mutation, the ratio was substantially and significantly reduced in the lenses of homozygotes (Figure 1E). In contrast, the ratio of P-p62(S349) to total p62 was significantly increased in lenses from homozygous Cx50D47A mice compared to that for the wild-type animals (Figure 1F); this ratio was not significantly different between wild-type and heterozygous Cx50D47A

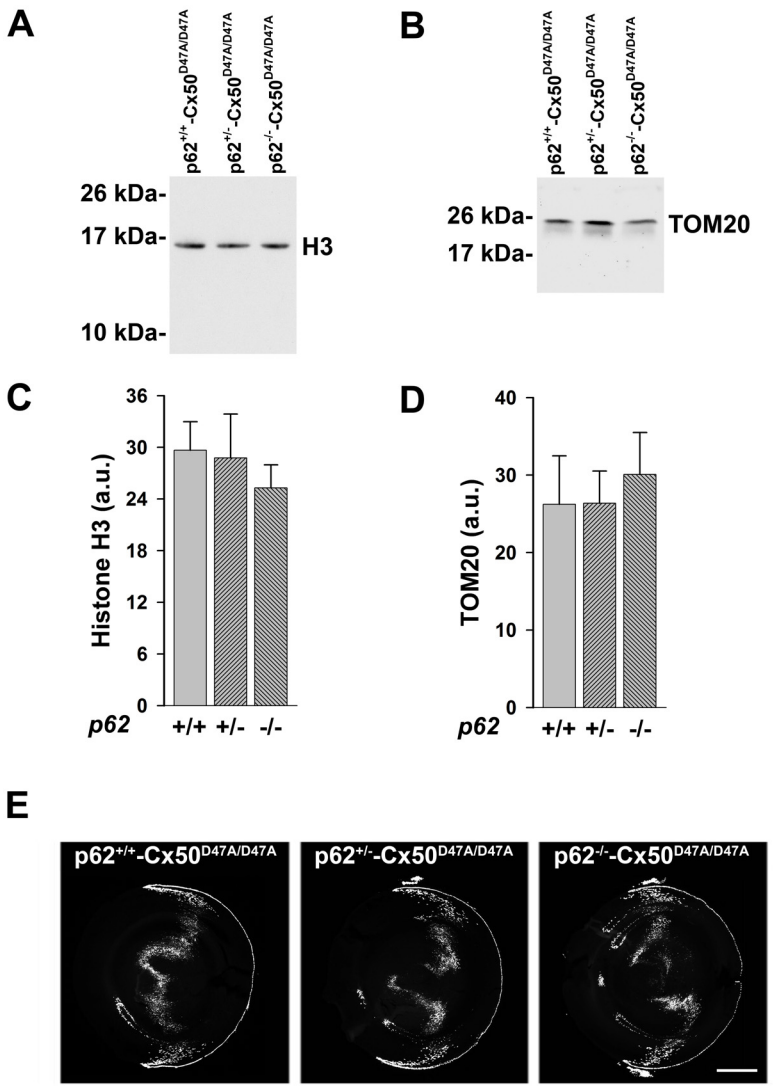

Figure 5. Deletion of *p62* in homozygous Cx50D47A lenses does not affect levels of nuclear and mitochondrial proteins or affect their impaired denucleation. **A**, **B**: Immunoblots of histone H3 (H3; **A**) and mitochondrial import receptor subunit TOM20 homolog (TOM20; **B**) in lens homogenates prepared from 1-month-old Cx50D47A homozygotes that were wild-type for *p62* (*p62*$^{+/+}$-Cx50$^{D47A/D47A}$) or heterozygous (*p62*$^{+/-}$-Cx50$^{D47A/D47A}$) or homozygous (*p62*$^{-/-}$-Cx50$^{D47A/D47A}$) *p62* null. The migration positions of the molecular mass markers are indicated on the left. **C, D**: The graphs show the densitometric quantification of the histone H3 (**C**) and TOM20 (**D**) immunoreactive bands in arbitrary units (a.u.). Data are presented as the mean (bar) + standard error of the mean obtained in three independent biologic replicates. **E**: Sections of lenses from 1-month-old Cx50D47A homozygotes that were wild-type for *p62* (*p62*$^{+/+}$-Cx50$^{D47A/D47A}$, left panel), or heterozygous (*p62*$^{+/-}$-Cx50$^{D47A/D47A}$, middle panel) or homozygous (*p62*$^{-/-}$-Cx50$^{D47A/D47A}$, right panel) *p62* null were stained with 4′,6-diamino-2-phenylindole dihydrochloride (DAPI) to detect nuclei and nuclear fragments. Scale bar: 300 µm.

lenses (Figure 1F). Thus, there is a specific decrease in phosphorylation of p62 at T269 or S272 and a specific increase in its phosphorylation at S349 in the homozygous Cx50 mutant lenses.

Deletion of p62 expression did not affect size or transparency of homozygous Cx50D47A lenses: To test the importance of p62 in the reduced growth and cataract formation in Cx50D47A lenses, we generated litters of mice that were homozygous for the Cx50D47A mutant allele and contained all three *p62* genotypes (wild-type and heterozygous and homozygous *p62* null) by breeding with *p62* null mice (which do not show lens abnormalities). We used immunoblotting to confirm the knockout of p62 in these animals. The immunoblots showed that p62 levels were significantly reduced (by more than 50%) in lenses of heterozygotes (p62$^{+/-}$-Cx50$^{D47A/D47A}$) compared with lenses from mice that were wild-type

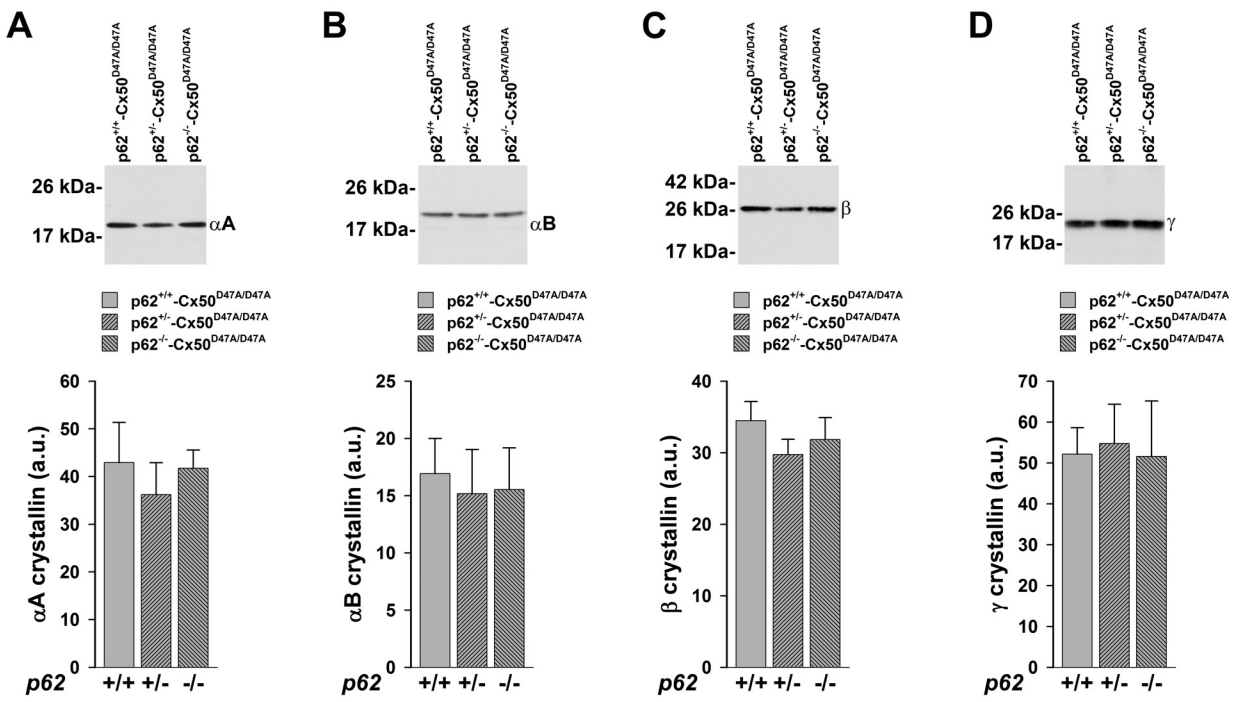

Figure 6. Deletion of *p62* does not alter levels of crystallins in homozygous Cx50D47A lenses. **A**–**D**: Top panels, immunoblots of αA (**A**), αB (**B**), β (**C**), and γ (**D**) crystallins in lens homogenates prepared from 1-month-old homozygous Cx50D47A mice that were wild-type for *p62* (*p62*$^{+/+}$-Cx50$^{D47A/D47A}$) or heterozygous (*p62*$^{+/-}$-Cx50$^{D47A/D47A}$) or homozygous (*p62*$^{-/-}$-Cx50$^{D47A/D47A}$) *p62* null. The migration positions of the molecular mass markers are indicated on the left. Bottom panels, the graphs show the quantification of the density of the immunoreactive bands of αA (**A**), αB (**B**), β (**C**) and γ (**D**) crystallins in arbitrary units (a.u.). Data are presented as the mean (bar) + standard error of the mean (n = 3 sets).

for p62 (p62$^{+/+}$-Cx50$^{D47A/D47A}$). p62 levels were undetectable in the lenses of homozygotes (p62$^{-/-}$-Cx50$^{D47A/D47A}$; Figure 2).

We examined the size, appearance, and transparency of the lenses of these mice by obtaining photomicrographs using dark-field illumination (Figure 3). All of these lenses appeared similar and contained cataracts regardless of their *p62* genotype (Figure 3A). The lenses did not differ in size, based on measurements of equatorial diameters (Figure 3B). There were no significant differences in the integrated densities of opacities between the cataracts in the lenses from p62$^{+/+}$-Cx50$^{D47A/D47A}$, p62$^{+/-}$-Cx50$^{D47A/D47A}$, and p62$^{-/-}$-Cx50$^{D47A/D47A}$ mice (Figure 3C). Thus, deletion of *p62* did not lead to a significant improvement or worsening of the growth or opacification of homozygous Cx50D47A lenses.

Deletion of p62 did not affect levels of lens fiber connexins in Cx50D47A mice: Among the intracellular functions of p62, it modulates different proteolytic pathways. Because Cx50D47A mice have low levels of both lens fiber connexins, we suspected that p62 might contribute to their degradation. To test this hypothesis, we evaluated the effects of *p62* deletion on levels of Cx46 and Cx50 by performing immunoblots for Cx46 (Figure 4A) and Cx50 (Figure 4B) on whole lens homogenates from p62$^{+/+}$-Cx50$^{D47A/D47A}$, p62$^{+/-}$-Cx50$^{D47A/D47A}$, and p62$^{-/-}$-Cx50$^{D47A/D47A}$ mice. Quantification of the levels of immunoreactive Cx46 (Figure 4A, bottom panel) and Cx50 (Figure 4B, bottom panel) did not show any significant differences between the Cx50D47A mice regardless of the *p62* genotype.

Deletion of p62 did not affect the levels of nuclear or mitochondrial proteins in the lenses of Cx50D47A mice: Because the lenses of Cx50D47A mice contain an increased abundance of nuclei and cellular organelles that are normally degraded during lens differentiation, we hypothesized that the elevation of p62 and the specific increase in its phosphorylation at S349 might reflect stimulation of autophagy in response to their impaired degradation. We determined the levels of histone H3 (one of the major proteins found in the chromatin of eukaryotic cell nuclei) and the mitochondrial import receptor subunit TOM20 homolog in whole lens homogenates of homozygous Cx50D47A mice that were wild-type for *p62* or heterozygous or homozygous for the deletion of *p62* (Figure 5A-D). Quantitation of the immunoblots showed that levels of

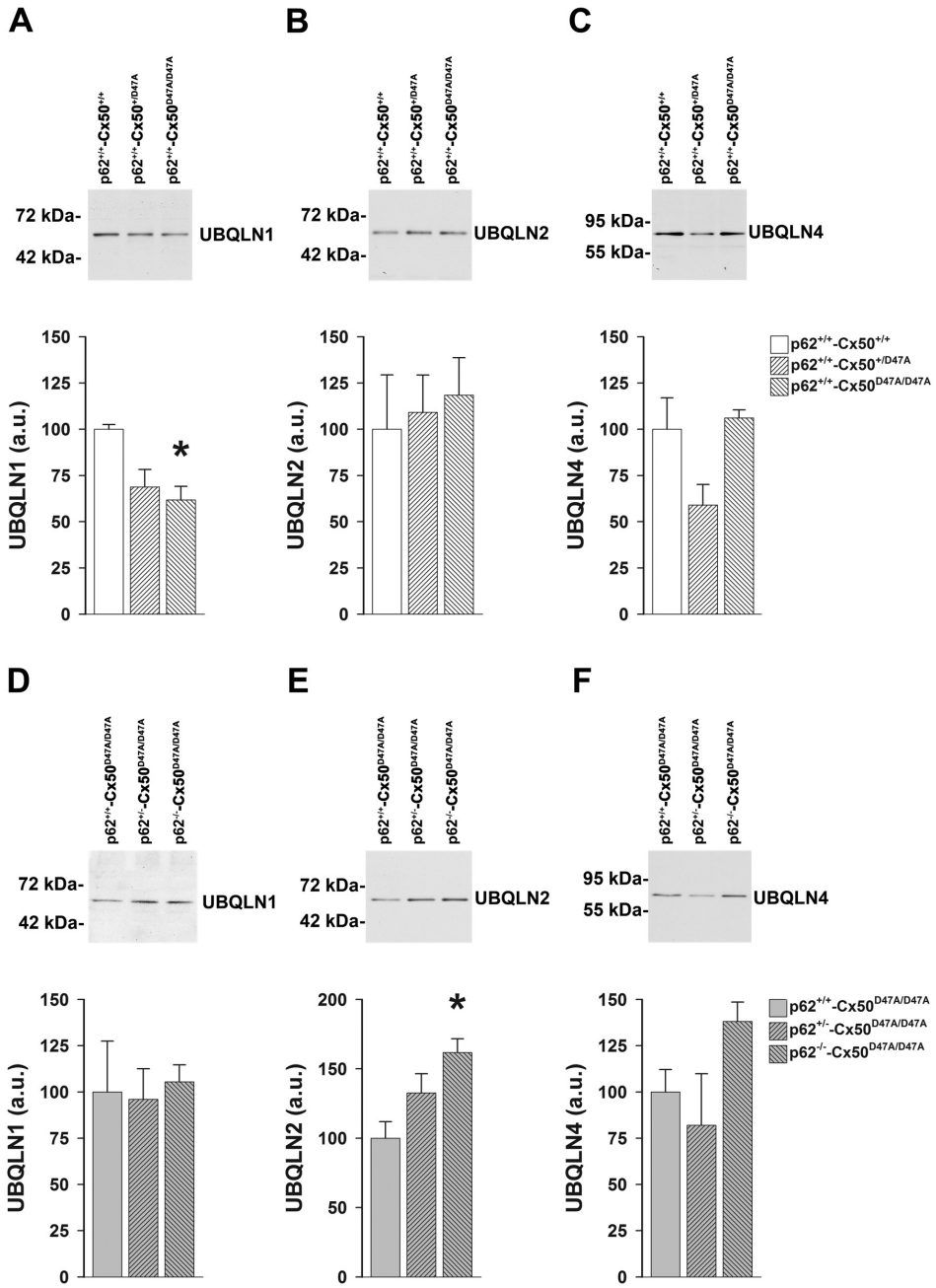

Figure 7. Levels of ubiquilins are altered in lenses of homozygous Cx50D47A mice with or without the deletion of p62. **A**–**C**: Immunoblots show levels of UBQLN1 (**A**), UBQLN2 (**B**), and UBQLN4 (**C**) in lens homogenates prepared from 1-month-old wild-type (*p62*$^{+/+}$-Cx50$^{+/+}$), or heterozygous (*p62*$^{+/+}$-Cx50$^{+/D47A}$) or homozygous (*p62*$^{+/+}$-Cx50$^{D47A/D47A}$) Cx50D47A mice. The migration positions of the molecular mass markers are indicated on the left. The graphs show the densitometric values of the immunoreactive ubiquilin bands. Data are presented as the mean (bar) + standard error of the mean (SEM; n = 3 sets) in arbitrary units (a.u.). **D**–**F**: Immunoblots show levels of UBQLN1 (**D**), UBQLN2 (**E**), and UBQLN4 (**F**) in lens homogenates prepared from 1-month-old homozygous Cx50D47A mice that were wild-type (*p62*$^{+/+}$-Cx50$^{D47A/D47A}$) or heterozygous (*p62*$^{+/-}$-Cx50$^{D47A/D47A}$) or homozygous (*p62*$^{-/-}$-Cx50$^{D47A/D47A}$) p62 null. The migration positions of the molecular mass markers are indicated on the left. The graphs show the densitometric values of the immunoreactive ubiquilin bands. Data are presented as the mean (bar) + SEM (n = 3 sets) in arbitrary units (a.u.). Asterisks denote statistically significant differences from wild-type lenses ($p<0.05$).

histone H3 and TOM20 did not differ significantly between the *p62* genotypes (Figure 5C,D). We also stained sections of $p62^{+/+}$-$Cx50^{D47A/D47A}$, $p62^{+/-}$-$Cx50^{D47A/D47A}$, and $p62^{-/-}$-$Cx50^{D47A/D47A}$ lenses with DAPI to detect nuclei and nuclear fragments; the DAPI staining did not appear different between the *p62* genotypes (Figure 5E).

Deletion of p62 did not alter the levels of crystallins in Cx50D47A lenses: Because p62 could be involved in the altered levels of crystallins that occur in many types of cataracts, including mice with connexin deletions or mutations [6,22,25], we examined levels of several crystallins by immunoblotting of lens homogenates (Figure 6). We found no significant differences in the levels of αA-, αB-, β-or γ-crystallins among the $p62^{+/+}$-$Cx50^{D47A/D47A}$, $p62^{+/-}$-$Cx50^{D47A/D47A}$, and $p62^{-/-}$-$Cx50^{D47A/D47A}$ lenses (Figure 6).

The lack of effect of p62 deletion could result from altered ubiquilin expression: Other proteins, like the ubiquilins, that act as adaptors and link proteolytic pathways [26] could potentially compensate for the lack of p62. Therefore, we performed immunoblots of whole lens homogenates to detect the levels of ubiquilins 1, 2, and 4 (UBQLN1, UBQLN2, and UBQLN4) [27].

We initially studied animals that were wild-type for p62 ($p62^{+/+}$) and had different Cx50D47A genotypes. The lenses of the heterozygous ($Cx50^{+/D47A}$) and homozygous Cx50D47A mice ($Cx50^{D47A/D47A}$) showed a decrease in UBQLN1 levels compared to wild-type mice; however, this difference reached statistical significance only for homozygotes that showed a 39% reduction in UBQLN1 levels (Figure 7A). The levels of UBQLN2 or UBQLN4 were not significantly different between the lenses of the $Cx50^{+/+}$, $Cx50^{+/D47A}$, and $Cx50^{D47A/D47A}$ mice (Figure 7 B,C).

Then, we studied mice that were homozygous for the Cx50D47A mutation and had different p62 genotypes. Heterozygous or homozygous deletion of *p62* did not affect the levels of UBQLN1 in the homozygous Cx50D47A lenses (Figure 7D). However, the levels of UBQLN2 were increased in the Cx50D47A lenses with homozygous (but not with heterozygous) deletion of *p62* (Figure 7E); it represented an 84% increase above the levels in the lenses from the Cx50D47A mice that were wild-type for p62 ($p62^{+/+}$-$Cx50^{D47A/D47A}$; Figure 7E). The levels of UBQLN4 were not significantly different among the homozygous Cx50D47A lenses of different p62 genotypes (Figure 7F).

DISCUSSION

In this study, we found that levels of total p62 were increased in homozygous Cx50D47A lenses. Increases in total p62 have been interpreted as indicating impaired autophagy in some systems, because p62 is degraded by autophagy, and it acts as a receptor that helps deliver ubiquitinated cargo (including protein aggregates and damaged mitochondria) to the autophagosome [28,29]. This interpretation has been invoked in studies of several mouse models of cataract, such as the R49C αA-crystallin and R120G αB-crystallin mutant mice [14,15]. However, Reneker and Chen [17] interpreted the increase in p62 in the lenses of mice expressing a dominant negative mutant fibroblast growth factor receptor as part of a compensatory response for autophagic degradation of the aggregates of ubiquitinated proteins formed in these lenses.

Autophagy plays a role in the lens [30,31], and a deletion or mutation of autophagy-associated proteins can lead to congenital or age-related cataracts [32,33]. However, several genes associated with autophagy (e.g., *Atg5*-Gene ID: 9474, *Pik3c3*-Gene ID: 225326, or *FIP200*- Gene ID: 12421) are not required for the normal programmed organelle degradation that occurs during lens cell differentiation [34]. Thus, although Cx50D47A lenses have impaired degradation of nuclei and mitochondria [6], it is unclear that their elevated levels of p62 result from impaired autophagy.

Our studies also showed that phosphorylation of p62 on T269/S272 was decreased in the lenses of homozygous Cx50D47A mice. Although phosphorylation of p62 has not previously been studied in relation to cataracts, there is an extensive literature regarding the roles of phosphorylation at these sites in other systems that may give some clues to their importance in Cx50D47A mice. Phosphorylation of p62 on T269/S272 during early mitosis facilitates entry into the cell cycle and exit from it [20]. Although it is not clear that there are abnormalities of cell cycle progression in the Cx50D47A mice, the smaller size of the mutant lenses compared with those of wild-type mice is consistent with reduced lens cell proliferation as seen in Cx50-null mice [35]. Thus, the decrease in T269/S272 phosphorylation could result in decreased mitosis in homozygous Cx50D47A lenses.

Phosphorylation of p62 at S349 was increased in the Cx50 mutant lenses. In other tissues, this modification stimulates an antioxidant response by increasing the binding affinity of p62 for Keap1 which decreases its interaction with Nrf2, allowing the stabilized Nrf2 to translocate to the nucleus and stimulate the expression of many antioxidant genes [10]. In cultured lens epithelial cells, Keap1/Nrf2 signaling is activated in response to stresses (including oxidation) [36,37], and treatment with sulforaphane causes translocation of Nrf2

to the nucleus [38]. Although levels of Nrf2 and its targets are altered in some studies of cataractous lenses [39,40], there is little information regarding the Nrf2-dependent activation of an antioxidant response (or reduced activation of an oxidant response) in intact lenses. Because oxidative damage to cellular components is involved in many different kinds of cataracts, it is reasonable to speculate that phosphorylation of p62 on S349 is part of a compensatory antioxidant response in Cx50D47A lenses.

Although p62 and its post-translationally modified forms may have a role in the lens, deletion of p62 expression in homozygous Cx50D47A lenses did not lead to any improvement or any worsening of their abnormalities. Lens size, opacities, connexin levels, crystallin levels, and levels of nuclear and mitochondrial proteins did not differ between lenses of Cx50D47A mice regardless of the presence or absence of p62. This suggests that p62 is not critical for development of the pathologies in the Cx50D47A mice and that it does not have a central role in a cellular response that limits the severity of the pathologies. These results might also reflect the redundancy of cellular systems. We considered that members of the ubiquilin family might compensate for the absence of p62, because these proteins also act as adaptors linking proteolytic pathways [40]. We found that homozygous deletion of p62 was accompanied by a significant increase in levels of ubiquilin 2 in lenses of homozygous Cx50D47A mice.

In summary, the lenses of homozygous Cx50D47A mice have increased levels of p62 and changes in phosphorylation of p62 at sites that have been associated with different cellular processes (e.g., autophagy, an antioxidant response, and regulation of mitosis). However, deletion of p62 expression does not significantly affect the pathologic changes (impaired differentiation and cataracts) of these lenses.

ACKNOWLEDGMENTS

This work was supported by National Institutes of Health Grant R01EY08368 (to ECB).

REFERENCES

1. Shiels A, Bennett TM, Hejtmancik JF. Cat-Map: putting cataract on the map. Mol Vis 2010; 16:2007-15. [PMID: 21042563].

2. Beyer EC, Ebihara L, Berthoud VM. Connexin mutants and cataracts. Front Pharmacol 2013; 4:43-[PMID: 23596416].

3. Berthoud VM, Ngezahayo A. Focus on lens connexins. BMC Cell Biol 2017; 18:6-[PMID: 28124626].

4. Favor J. A comparison of the dominant cataract and recessive specific-locus mutation rates induced by treatment of male mice with ethylnitrosourea. Mutat Res 1983; 110:367-82. [PMID: 6877261].

5. Steele EC, Lyon MF, Favor J, Guillot PV, Boyd Y, Church RL. A mutation in the connexin 50 (Cx50) gene is a candidate for the *No2* mouse cataract. Curr Eye Res 1998; 17:883-9. [PMID: 9746435].

6. Berthoud VM, Minogue PJ, Yu H, Schroeder R, Snabb JI, Beyer EC. Connexin50D47A decreases levels of fiber cell connexins and impairs lens fiber cell differentiation. Invest Ophthalmol Vis Sci 2013; 54:7614-22. [PMID: 24204043].

7. Berthoud VM, Minogue PJ, Lambert PA, Snabb JI, Beyer EC. The cataract-linked mutant connexin50D47A causes endoplasmic reticulum stress in mouse lenses. J Biol Chem 2016; 291:17569-78. [PMID: 27317663].

8. Jara O, Minogue PJ, Berthoud VM, Beyer EC. Chemical chaperone treatment improves levels and distributions of connexins in Cx50D47A mouse lenses. Exp Eye Res 2018; 175:192-8. [PMID: 29913165].

9. Berthoud VM, Gao J, Minogue PJ, Jara O, Mathias RT, Beyer EC. The connexin50D47A mutant causes cataracts by calcium precipitation. Invest Ophthalmol Vis Sci 2019; 60:2336-46. [PMID: 31117126].

10. Komatsu M, Kurokawa H, Waguri S, Taguchi K, Kobayashi A, Ichimura Y, Sou Y, Ueno I, Sakamoto A, Tong KI, Kim M, Nishito Y, Iemura S, Natsume T, Ueno T, Kominami E, Motohashi H, Tanaka K, Yamamoto M. The selective autophagy substrate p62 activates the stress responsive transcription factor Nrf2 through inactivation of Keap1. Nat Cell Biol 2010; 12:213-23. [PMID: 20173742].

11. Duran A, Amanchy R, Linares JF, Joshi J, Abu-Baker S, Porollo A, Hansen M, Moscat J, Diaz-Meco MT. p62 is a key regulator of nutrient sensing in the mTORC1 pathway. Mol Cell 2011; 44:134-46. [PMID: 21981924].

12. Rogov V, Dötsch V, Johansen T, Kirkin V. Interactions between autophagy receptors and ubiquitin-like proteins form the molecular basis for selective autophagy. Mol Cell 2014; 53:167-78. [PMID: 24462201].

13. Sánchez-Martín P, Komatsu M. p62/SQSTM1 - steering the cell through health and disease. J Cell Sci 2018; 131:1-13. [PMID: 30397181].

14. Wignes JA, Goldman JW, Weihl CC, Bartley MG, Andley UP. p62 expression and autophagy in αB-crystallin R120G mutant knock-in mouse model of hereditary cataract. Exp Eye Res 2013; 115:263-73. [PMID: 23872361].

15. Andley UP, Goldman JW. Autophagy and UPR in alpha-crystallin mutant knock-in mouse models of hereditary cataracts. Biochim Biophys Acta 2016; 1860:234-9. [PMID: 26071686].

16. Zhou Y, Bennett TM, Shiels A. Lens ER-stress response during cataract development in *Mip*-mutant mice. Biochim Biophys Acta 2016; 1862:1433-42. [PMID: 27155571].

17. Reneker LW, Chen H. Protein aggregate formation and SQSTM1/p62 induction in the transgenic mouse lens

expressing dominant negative mutant FGFR. Invest Ophthalmol Vis Sci 2011; 52:3927-abstract.

18. Lichtenstein A, Gaietta GM, Deerinck TJ, Crum J, Sosinsky GE, Beyer EC, Berthoud VM. The cytoplasmic accumulations of the cataract-associated mutant, Connexin50P88S, are long-lived and form in the endoplasmic reticulum. Exp Eye Res 2009; 88:600-9. [PMID: 19073179].
19. Ichimura Y, Waguri S, Sou Y-S, Kageyama S, Hasegawa J, Ishimura R, Saito T, Yang Y, Kouno T, Fukutomi T, Hoshii T, Hirao A, Takagi K, Mizushima T, Motohashi H, Lee MS, Yoshimori T, Tanaka K, Yamamoto M, Komatsu M. Phosphorylation of p62 activates the Keap1-Nrf2 pathway during selective autophagy. Mol Cell 2013; 51:618-31. [PMID: 24011591].
20. Linares JF, Amanchy R, Greis K, Diaz-Meco MT, Moscat J. Phosphorylation of p62 by cdk1 controls the timely transit of cells through mitosis and tumor cell proliferation. Mol Cell Biol 2011; 31:105-17. [PMID: 20974803].
21. Berthoud VM, Minogue PJ, Guo J, Williamson EK, Xu X, Ebihara L, Beyer EC. Loss of function and impaired degradation of a cataract-associated mutant connexin50. Eur J Cell Biol 2003; 82:209-21. [PMID: 12800976].
22. Berthoud VM, Minogue PJ, Yu H, Snabb JI, Beyer EC. Connexin46fs380 causes progressive cataracts. Invest Ophthalmol Vis Sci 2014; 55:6639-48. [PMID: 25103261].
23. Minogue PJ, Beyer EC, Berthoud VM. CHOP is dispensable for lens transparency in wild-type and connexin50 mutant mice. Mol Vis 2019; 25:535-45. [PMID: 31908399].
24. Komatsu M, Waguri S, Koike M, Sou Y-S, Ueno T, Hara T, Mizushima N, Iwata J, Ezaki J, Murata S, Hamazaki J, Nishito Y, Iemura S, Natsume T, Yanagawa T, Uwayama J, Warabi E, Yoshida H, Ishii T, Kobayashi A, Yamamoto M, Yue Z, Uchiyama Y, Kominami E, Tanaka K. Homeostatic levels of p62 control cytoplasmic inclusion body formation in autophagy-deficient mice. Cell 2007; 131:1149-63. [PMID: 18083104].
25. Gong X, Li E, Klier G, Huang Q, Wu Y, Lei H, Kumar NM, Horwitz J, Gilula NB. Disruption of *α3* connexin gene leads to proteolysis and cataractogenesis in mice. Cell 1997; 91:833-43. [PMID: 9413992].
26. Komatsu M, Kageyama S, Ichimura Y. p62/SQSTM1/A170: physiology and pathology. Pharmacol Res 2012; 66:457-62. [PMID: 22841931].
27. Marín I. The ubiquilin gene family: evolutionary patterns and functional insights. BMC Evol Biol 2014; 14:63-[PMID: 24674348].
28. Moscat J, Diaz-Meco MT, Wooten MW. Signal integration and diversification through the p62 scaffold protein. Trends Biochem Sci 2007; 32:95-100. [PMID: 17174552].
29. Morishita H, Mizushima N. Autophagy in the lens. Exp Eye Res 2016; 144:22-8. [PMID: 26302409].
30. Costello MJ, Brennan LA, Basu S, Chauss D, Mohamed A, Gilliland KO, Johnsen S, Menko S, Kantorow M. Autophagy and mitophagy participate in ocular lens organelle degradation. Exp Eye Res 2013; 116:141-50. [PMID: 24012988].
31. Morishita H, Eguchi S, Kimura H, Sasaki J, Sakamaki Y, Robinson ML, Sasaki T, Mizushima N. Deletion of autophagy-related 5 (*Atg5*) and *Pik3c3* genes in the lens causes cataract independent of programmed organelle degradation. J Biol Chem 2013; 288:11436-47. [PMID: 23479732].
32. Chen J, Ma Z, Jiao X, Fariss R, Kantorow WL, Kantorow M, Pras E, Frydman M, Pras E, Riazuddin S, Riazuddin SA, Hejtmancik JF. Mutations in *FYCO1* cause autosomal-recessive congenital cataracts. Am J Hum Genet 2011; 88:827-38. [PMID: 21636066].
33. Matsui M, Yamamoto A, Kuma A, Ohsumi Y, Mizushima N. Organelle degradation during the lens and erythroid differentiation is independent of autophagy. Biochem Biophys Res Commun 2006; 339:485-9. [PMID: 16300732].
34. Sellitto C, Li L, White TW. Connexin50 is essential for normal postnatal lens cell proliferation. Invest Ophthalmol Vis Sci 2004; 45:3196-202. [PMID: 15326140].
35. Elanchezhian R, Palsamy P, Madson CJ, Mulhern ML, Lynch DW, Troia AM, Usukura J, Shinohara T. Low glucose under hypoxic conditions induces unfolded protein response and produces reactive oxygen species in lens epithelial cells. Cell Death Dis 2012; 3:e301-[PMID: 22513875].
36. Elanchezhian R, Palsamy P, Madson CJ, Lynch DW, Shinohara T. Age-related cataracts: homocysteine coupled endoplasmic reticulum stress and suppression of Nrf2-dependent antioxidant protection. Chem Biol Interact 2012; 200:1-10. [PMID: 22964297].
37. Liu H, Smith AJO, Lott MC, Bao Y, Bowater RP, Reddan JR, Wormstone IM. Sulforaphane can protect lens cells against oxidative stress: implications for cataract prevention. Invest Ophthalmol Vis Sci 2013; 54:5236-48. [PMID: 23812493].
38. Whitson JA, Wilmarth PA, Klimek J, Monnier VM, David L, Fan X. Proteomic analysis of the glutathione-deficient LEGSKO mouse lens reveals activation of EMT signaling, loss of lens specific markers, and changes in stress response proteins. Free Radic Biol Med 2017; 113:84-96. [PMID: 28951044].
39. Gao Y, Yan Y, Huang T. Human age-related cataracts: epigenetic suppression of the nuclear factor erythroid 2-related factor 2-mediated antioxidant system. Mol Med Rep 2015; 11:1442-7. [PMID: 25370996].
40. Lee DY, Brown EJ. Ubiquilins in the crosstalk among proteolytic pathways. Biol Chem 2012; 393:441-7. [PMID: 22628307].

Articles are provided courtesy of Emory University and the Zhongshan Ophthalmic Center, Sun Yat-sen University, P.R. China. The print version of this article was created on 18 March 2020. This reflects all typographical corrections and errata to the article through that date. Details of any changes may be found in the online version of the article.